The use of *Brugmansia arborea* as a green corrosion inhibitor for AISI 1018 carbon steel in acid media

Adriana Rodríguez Torres, María Guadalupe Valladares Cisneros, Jorge Uruchurtu Chavarín, Cecilia Cuevas Arteaga & María Aurora Veloz Rodríguez

Taylor & Francis
Taylor & Francis Group

REVIEW

🔓 OPEN ACCESS | Check for updates

The use of *Brugmansia arborea* as a green corrosion inhibitor for AISI 1018 carbon steel in acid media

Adriana Rodríguez Torres[a], María Guadalupe Valladares Cisneros[b], Jorge Uruchurtu Chavarín[c], Cecilia Cuevas Arteaga[c] and María Aurora Veloz Rodríguez[a]

[a]Academic Area of Earth Sciences and Materials, Institute of Basic Sciences and Engineering, Autonomous University of Hidalgo State, Pachuca de Soto, México; [b]School of Chemical Sciences and Engineering, Autonomous University of Morelos State, Morelos, México; [c]Research Center for Engineering and Applied Sciences, Autonomous University of Morelos State, Morelos, México

ABSTRACT

This study shows the inhibitory activity of the hexane, acetone and methanol extracts of *Brugmansia arborea* (*B. arborea*) during the corrosion of 1018 steel in 0.5 M of H_2SO_4. This was carried out by electrochemical impedance spectroscopy (EIS) and potentiodynamic polarization curves (PDP) techniques. The maximum efficiency for the three extracts was registered with 400 and 500 ppm concentrations, obtaining 98% by EIS and 80% by PDP. Through PDP, an inhibition behavior of the cathodic type was determined. During the residence time test, *B. arborea* reached a maximum inhibition efficiency of 98% at 24 h with acetone extract and at 20 h with methanol extract. The compound's chemical structure present in *B. arborea* was analyzed by the Fourier Transform infrared spectroscopy technique, and the presence of functional groups such as the amines was observed. The reason why an inhibitory activity is attributed to these compounds is because they contain nitrogen that may easily form complexes that are strongly adsorbed creating a thin layer on the metallic surface.
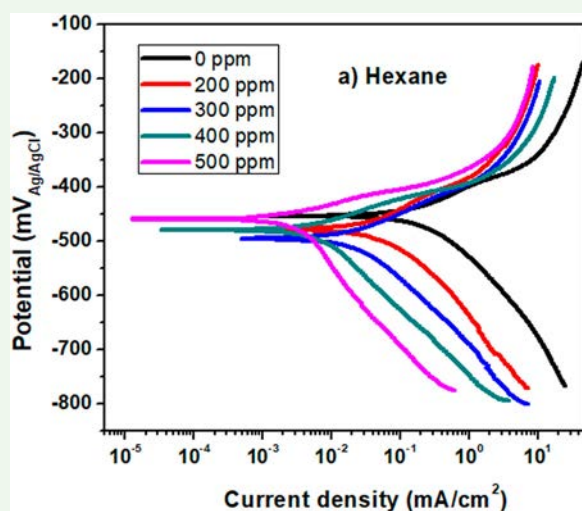
1. Introduction

Economically, the expenses due to corrosion are estimated at around 5-7% of the annual gross domestic product of a country (*1*). As time has passed, there have been improved techniques and methods for corrosion protection. However, the losses are not decreasing due to the constantly increasing pollution in the atmosphere and the technological processes that impose sterner operation conditions (*2*). Industry uses acid solutions for different processes, such as the chemical scaling. However, they are aggressive to metals; therefore, the use of organic inhibitors is predominant and necessary. Due to the good efficiency in corrosion protection, those inhibitors that contain in their chemical structures nitrogen as a heteroatom, such as amines, imidazolines, pyrimidines, etc. (*3*, *4*) were preferred.

As well inhibitors that include more than nitrogen atoms in their chemical structure (*5*, *6*), including oxygen (*7*) or sulfur (*8*) which already exist for steel protection of acid media.

It is common to be mentioned in several studies that organic inhibitors produce adequate inhibition efficiencies for corrosion, containing heteroatoms in their structure and it is through the pairs of free electrons, that these inhibitors can be adsorbed on the metallic surface and form chelate type complexes, giving, as a result, the formation of a thin layer on the metallic surface that contribute preventing the corrosion and the metal dissolution (*9*). Unfortunately, some of these efficient corrosion inhibitors turned out to be toxic, affecting human health and generating negative environmental impact, thus the environmental laws each day are stricter in the matter. This situation has motivated to search and analyze natural sources that are able to provide efficient chemical compounds as inhibitors, that at the same time, are less toxic or even better eco-friendly.

In the natural field, vegetal species have been explored, such as leaves (*10*), cortex (*11*), fruit (*12*), shell (*13*), etc., as green corrosion inhibitors for carbon steel in acid media through electrochemical techniques. Al-Fakih reported the inhibitory activity of the corrosion by using turmeric and ginger, for mild steel in acid media (*14*). They determined maximum inhibition efficiencies of 92% and 91% respectively. Also, it has been reported the use of *Allium sativum* obtaining corrosion inhibition efficiencies of 96% for 1018 steel (*15*). By the use of *Rhus verniciflua,* Prabakaran reported an efficiency of 93% (*16*). Haldhar using *Valeriana wallichii* proved an efficiency of 93% (*17*). Another research about Rubber leaves showed the corrosion inhibition of mild steel in acid media obtaining an efficiency of 86% (*18*), among others.

With these data, it can be observed that different species are studied; however, it is necessary to continue improving the knowledge generation about the natural inhibitors field. Thus, the present research is oriented to the study of corrosion inhibition of 1018 steel in sulfuric acid with *Brugmansia arborea.*

Brugmansia arborea is commonly known in Mexico as Floripondio, it is a native plant of South America and it belongs to the *Solanaceae* family (*19*). This family is known for producing alkaloids, tropane particularly, which is widely used in traditional medicine due to its anticholinergic properties (*20*). Figure 1 shows some of the chemical compounds that have been reported for *B. arborea,* which are: hyoscyamine (**I**), anisodamine (**II**) and scopolamine (**III**); this last compound is considered of great commercial value due to its pharmacological activity and minor side effects (*21*). Some heteroatoms such as N and O, as well as the presence of π-electrons in carbon–carbon double bonds in the chemical compounds of *B. arborea,* make it a potential corrosion inhibitor. Therefore, in the present work, extract of *B. arborea* with acetone, hexane and methanol was tested as corrosion inhibitor of 1018 steel in acid media.

Carbon steel AISI 1018 is widely used as a construction material in many industries due to its excellent mechanical properties and low cost (*22*), thus, the evaluation of this steel can contribute important and useful information to the corrosion control field in industries.

2. Methodology

Electrochemical tests were carried out with AISI 1018 steel cylindrical probes of 3 cm high×0.635 cm diameter, with a weight percentage composition of: 0.14-0.2% carbon, 0.6-0.9% manganese, a maximum of 0.04% phosphor, a maximum of 0.05% sulfur and the remaining 98.81-99.26 iron. Samples were encapsulated in commercial epoxy resin, which is used for corrosion protection in almost all of the surface, leaving a defined contact area of 0.316 cm^2. Each of the samples was sanded with carbide silicon paper from 100 to 1000 grade, to obtain a homogenous surface.

2.1. Green inhibitor

Brugmansia arborea (B. arborea) leaves were collected in Chamilpa village, which is in Morelos, Mexico. They were submitted to a drying process at a constant temperature of 30 °C, with light absence. The leaves were triturated, weighted (1.35 kg) and collocated in a 4-liter flask to proceed to macerate them with different solvents: hexane, acetone and methanol during 72 h each one. After this time, the solution was filtered and
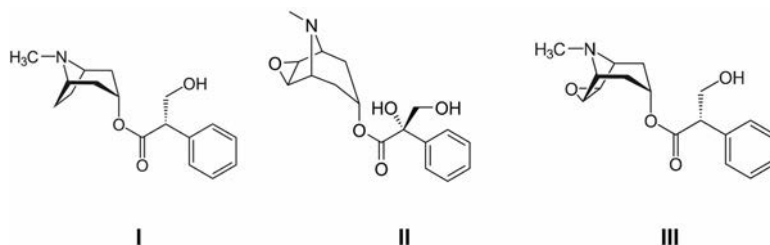

Figure 1. Chemical compounds present in *Brugmansia arborea.*

concentrated using a rotary evaporator BUCHI branch to eliminate the solvent. Finally, the quantities of extracts obtained were 1.77 g of hexane, 5.77 g of acetone and 9.72 g of methanol. They were evaluated as inhibitors in the concentration range between 200–500 ppm.

2.2. Aggressive solution

A solution with sulfuric acid at 98% analytical grade and deionized water to obtain a concentration of 0.5 M H_2SO_4 was used as an aggressive medium to assess the effects with different concentrations of *B. arborea* as corrosion inhibitor of 1018 steel.

2.3. Electrochemical evaluation

The electrochemical techniques used for the evaluation of the different *B. arborea* extracts as corrosion inhibitor were electrochemical impedance spectroscopy (EIS) and polarization potentiodynamic curves (PDP). During the measurements, a conventional three-electrode cell was used, with 1018 carbon steel as a working electrode, Ag/AgCl as a reference electrode and a graphite counter electrode. Every test was performed three times, after 10 min of 1018 steel electrode immersion, when it reached a stable open circuit potential value. PDP measurements were carried out with a speed rate of 1 mV/s in an interval of ±250 mV from the corrosion potential. The corrosion current density values I_{corr}, were obtained using Tafel extrapolation. The inhibition efficiency (η) was calculated according to Equation (1):

$$\eta(\%) = \left[\frac{i_{corr1} - i_{corr2}}{i_{corr1}}\right] * 100 \qquad (1)$$

where i_{corr1} and i_{corr2} are the current density without and with inhibitor respectively.

EIS tests were carried out with signal amplitude of 10 mV and a frequency interval between 0.01–10,000 Hz in an ACM instruments GillAC potentiostat.

2.4. Infrared spectroscopy using Fourier transforms. (FTIR)

Additionally, FTIR analysis was performed to determine the functional groups of the present compounds for *B. arborea*. The tests were carried out with Alpha spectrometer and Opus software.

2.5. Toxicity bioassay using Lactuca sativa (L. sativa) seeds

The phytotoxic effect of *B. arborea* extracts was observed through an acute toxicity bioassay by germinating

L. sativa seeds and seedlings growth. Following the method stablished by Sobrero and Ronco (*23*), pesticide-free *L. sativa* seeds from "Rancho los Molinos" in Morelos, Mexico, were used. Ten seeds were deposited inside a Petri cage on a filter paper previously saturated with the different concentrations of extract (200–500 ppm). A positive control of 0.2 M $ZnSO_4$ and a negative control of mineral water were used. Petri cages were placed inside of hermetic bags to preserve a humid environment and they were conserved for 120 h in light absence and at constant temperature of (24 ± 2 °C). At the end of this time, the germinated seed was dried and lengths of its radicle and hypocotyl reached with each concentration registered. Every test was done three times to ensure the reproducibility of the results.

3. Results and discussion

3.1. Potentiodynamic polarization curves

Figure 2 shows the potentiodynamic polarization curves for 1018 steel in acid medium with and without *B. arborea* different concentrations of hexane, acetone and methanol extracts. In the potential range used, for the three extracts, no formation of passive films was observed. This can happen because during the corrosion process, as *B. arborea* inhibitor is present, the formation and the redissolution of corrosion products and/or inhibitor molecules occurs and maintain the surface active (*24, 25*). At the moment the inhibitor was added, the corrosion potential was displaced to more negative values. This variation indicates that *B. arborea* extracts may act as a cathodic inhibitor in the hydrogen evolution (*26*). While inhibitor concentration increases, the anodic and cathodic branches are displaced to lower current density values, showing that inhibitor molecules could be adsorbed on the metal surface (*27, 28*).

In Table 1, the calculated values through Tafel extrapolation are shown: current density (I_{corr}), corrosion potential (E_{corr}), anodic slope (β_a), cathodic slope (β_c) and corrosion rate (V_{corr}). It can be observed that, by adding inhibitor concentration, current density and corrosion rate decrease as the efficiency increases, obtaining a maximum efficiency of 90% for hexane extract, 80% for acetone and 83% for methanol extracts.

3.2. Electrochemical impedance spectroscopy

Figure 3 shows Nyquist diagrams obtained through EIS technique for corrosion inhibition of 1018 steel in acid media using different extracts of *B. arborea,* at 25 ± 2 °C. In the three cases, the behavior observed is different from perfect semicircles, which is attributed to a deviation of
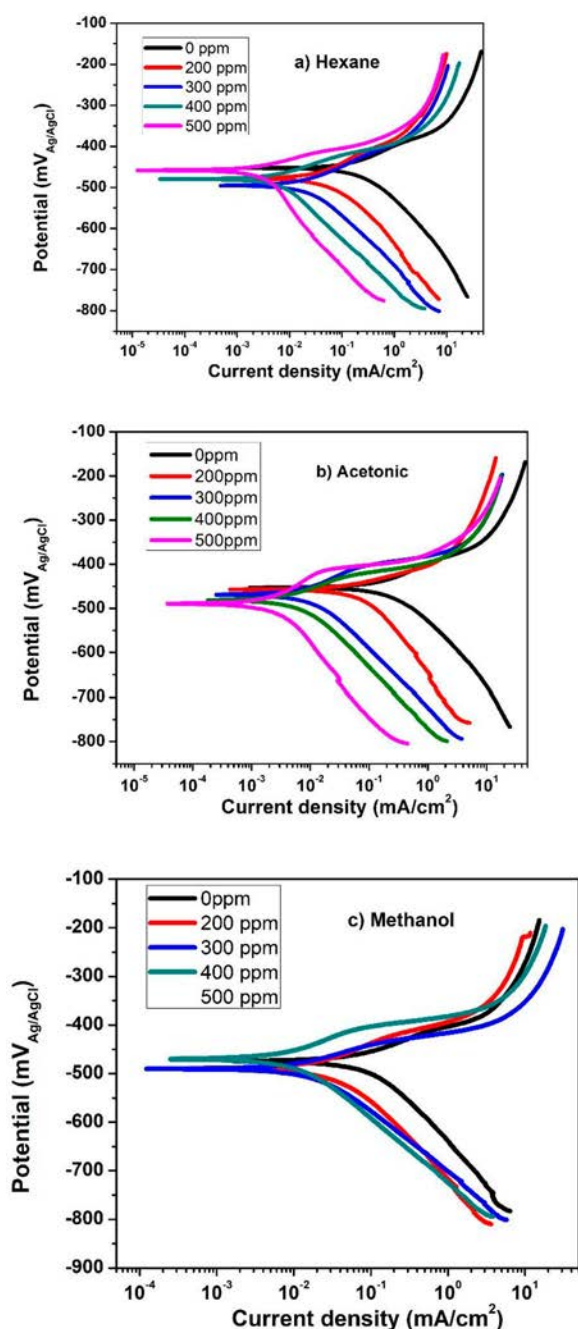
Figure 2. Concentration effect of *B. arborea extracts:* (a) hexane, (b) acetone and (c) methanol by doing polarization curves for 1018 steel in 0.5 M H$_2$SO$_4$.

Table 1. Electrochemical polarization parameters for AISI 1018 carbon steel in 0.5 M of H$_2$SO$_4$ as a function of *B. arborea* concentration at 25°C.

Extract	C_{inh} [ppm]	β_a [mV/ dec]	β_c [mV/ dec]	Restpot E_{corr} [mV]	I_{corr} [mA/ cm^2]	V_{corr} [mm/ year]	% η
Hexane	0	62	111	−454	2.2	26.21	–
	200	53	138	−471	0.7	8.13	68
	300	65	131	−493	0.36	4.11	84
	400	42	119	−481	0.42	4.89	80
	500	33	136	−462	0.2	2.37	90
Acetone	200	54	164	−458	0.49	5.62	78
	300	53	118	−470	0.58	6.7	74
	400	41	138	−482	0.44	5.21	80
	500	48	138	−487	0.44	5.1	80
Methanol	200	51	140	−462	0.8	9.3	64
	300	39	123	−791	0.70	8.2	68
	400	67	159	−489	0.38	4.5	83
	500	43	139	−470	0.48	5.7	78

the 1018 steel electrode surface respect to the ideal capacitive behavior, because of the non-homogeneous surface that allows the distribution of active sites and/or the adsorption of the inhibitor molecules (*29, 30*). Also, two capacitive semicircles are observed: the first, is formed at high frequencies and can be attributed to the charge transfer resistance, which corresponds to the resistance between the 1018 electrode surface and the Helmholtz external plane; the second capacitive semicircle formed at low frequencies is attributed to the resistance of a layer formed by the inhibitor; which is

generated due to molecules adsorption onto the metal surface. This event has been compatible with many studies in literature (*31–33*). As a result of the inhibitor adsorption, the semicircle diameter increased as the inhibitor concentration increased in the medium.

In Figure 4, the obtained equivalent circuit is shown; where R_s is the solution resistance, R_{ct} is the charge transfer resistance, *CPE* is the constant phase element to model the condenser non-ideality and R_f corresponds to the resistance given by the inhibitor layer and/or by the corrosion products (*34*). This type of circuit suppose that the inhibitor forms a faulty layer onto the metal, acting as an effective obstacle before the aggressive media of the acid solution, that is why the corrosion process is controlled by a mechanism that occurs in the non-protected metal, with a much reduced active surface, this type of circuit has been used in many studies to analyze EIS obtained data by other inhibitors in which a second capacitive semicircle is formed (*35–40*).

Impedance associated values Z_{CPE} can be calculated from Equation (2):

$$Z_{CPE} = \frac{1}{Q(j\omega)^n} \tag{2}$$

where Q is the pseudo capacitance, j the current density, ω is the angular frequency and n is a heterogeneity indicator or surface roughness. Depending on n value, Z_{CPE} can be represented as ($Z_{CPE} = R$, $n = 0$), capacitance ($Z_{CPE} = C$, $n = 1$), Warburg Impedance ($Z_{CPE} = W$, $n = 0.5$) or inductance ($Z_{CPE} = L$, $n = −1$), (*41*).

The double layer capacitance value (CPE_{dl}) can be calculated according Equation (3) (*42*):

$$CPE_{dl} = (QR_p^{1-n})^{\frac{1}{n}} \tag{3}$$

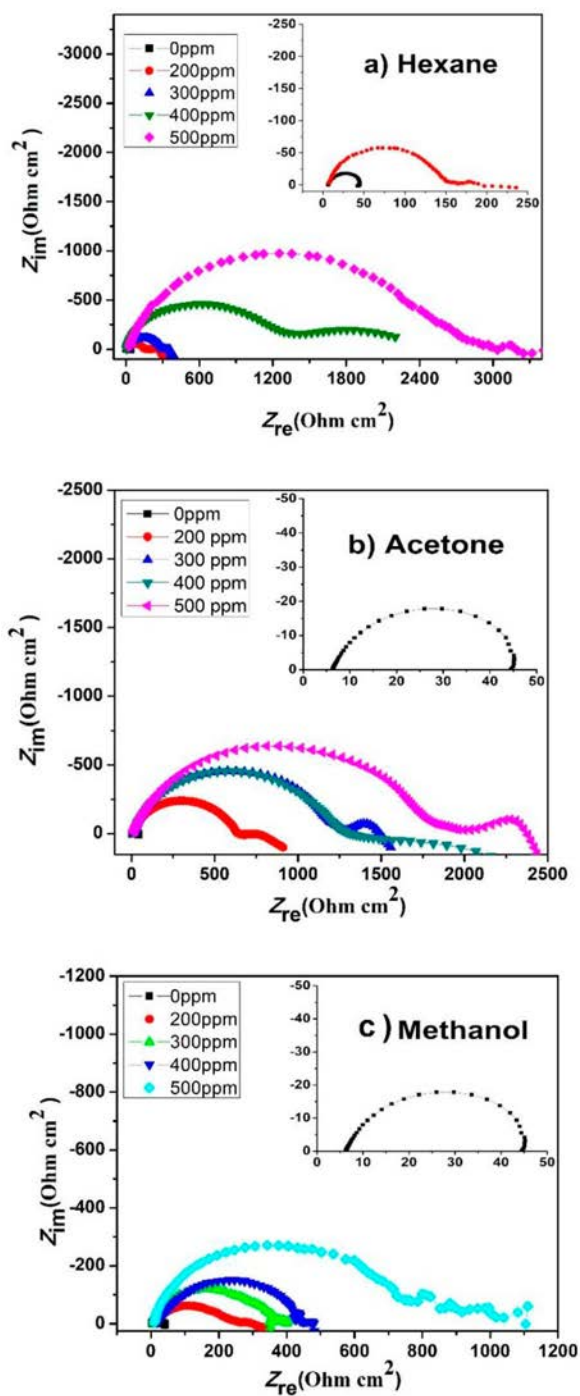Extracts efficiency inhibition (η) as corrosion inhibitor for

Figure 3. *B. arborea* extracts concentration effect: (a) hexane, (b) acetone and (c) methanol by EIS for 1018 carbon steel in 0.5 M H_2SO_4.

1018 steel was calculated through Equation (4):

$$\eta\% = 100 \frac{R_{ct1} - R_{ct2}}{R_{ct2}} \qquad (4)$$

where R_{ct1} and R_{ct2} are the charge transfer with and without inhibitor, respectively.

In Table 2 it can be observed the obtained data from the electric circuit simulation with the different

B. arborea extract concentrations as corrosion inhibitor for 1018 steel in acid media. The surface coverture grade was calculated using Equation (5):

$$\theta = \frac{\eta}{100} \qquad (5)$$

It can be appreciated that by increasing the inhibitor concentration, the double layer capacitance values (C_{dl}) decrease due to an increase in the electric double layer thickness; which suggest that the present molecules in the different inhibitors are adsorbed onto the surface, displacing the present molecules in the aggressive medium (*43,44*).

It was observed in PDP and by EIS that by increasing the inhibition concentration, the resistance increases, at the same time as the efficiency. The efficiencies registered by PDP are slightly lower than EIS's, this is due to during PDP it was applied a potential of ±250 mV displacing the equilibrium of the reaction. However, in both of the electrochemical techniques, the maximum efficiency for the three extracts were obtained at 400 and 500 ppm concentrations.

Acetone and methanol extracts were considered for residence time evaluation; the hexane extract was ignored due to its insolubility in aqueous-media.

Figure 5 shows Nyquist diagrams according to the residence time for acetone and methanol extracts, both at a 500 ppm concentration. It can be observed an inductive ripple at low frequencies, it is associated to adsorption and desorption processes of species present in the medium (*45*); also, it is observed how the semicircle diameter of the Nyquist diagrams increases, reaching the maximum at 24 h for acetone and at 20 h for methanol extract. This is attributed to a process in which inhibitor molecules are being adsorbed onto the metal surface by forming chemical interactions of chelate type. After this time, the semicircle diameter begins to decrease and at 30 h reaches the same resistance than at 0 h, this could be possible due to the existence of a desorption process of the chelate complexes formed with the inhibitor that occurs at higher velocities than the protection rate (*46*).

Other researches have obtained good efficiencies with vegetal species (*47–50*); however, its efficiency decreases rapidly with the time-pass; some other even not consider relevant the residence study. By comparing *B. arborea* with other vegetal extracts, it can be distinguished as can reach a maximum efficiency at 24 h and it maintains over the 80% until 30 h.

3.3. Adsorption isotherms

In order to know the corrosion mechanics, it was necessary to evaluate the adsorption isotherms, as they can
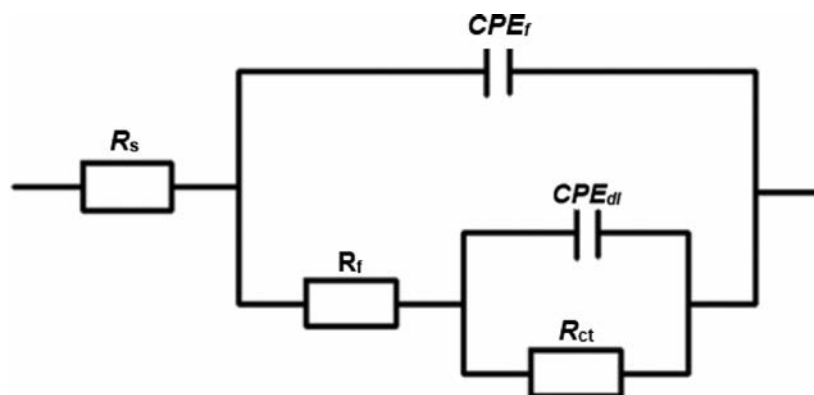
Figure 4. Equivalent circuit used for data fitting obtained by EIS from *Brugmansia arborea* as green corrosion inhibitor for AISI 1018 carbon steel in acid media.

Table 2. Effect of *B. arborea* concentration on the electrochemical parameters obtained from EIS measurements.

B. arborea extract	C_{inh} [ppm]	R_s Ω cm^2	R_{ct} Ω cm^2	R_f Ω cm^2	CPE_{dl} μF cm^{-2}	CPE_f μF cm^{-2}	θ	η%
Hexane	0	6	45	-	53	-	-	–
	200	4.4	160	80	26.3	224	0.72	72
	300	44	301	84	17.8	107	0.85	85
	400	4	1256	970	18.2	278	0.96	**96**
	500	11	2580	772	8.12	240	0.98	**98**
Acetone	200	10	662	254	16.2	450	0.93	93
	300	11	1200	312	12.7	365	0.96	96
	400	13	1273	867	8.85	510	0.96	**96**
	500	12	1779	594	9.88	217	0.98	97
Methanol	200	8	247	92	156	4151	0.82	82
	300	18	369	44	47.9	1399	0.88	88
	400	9	450	43	62.8	470	0.90	**90**
	500	3	752	349	36.1	535	0.94	**94**

provide information related to adsorption process characteristics. So, there were evaluated three different adsorption models: Temkin, Langmuir and Frumkin, obtaining the better fit with the last one. In Figure 6, Frumkin isotherms for *B. arborea* acetone and methanol extracts are shown, which were calculated following Equation (6):

$$\log \frac{\theta C_{inh}}{1 - \theta} = \log K + g\theta \qquad (6)$$

where C_{inh} is the inhibitor concentration, K is the equilibrium constant of adsorption and desorption and g corresponds to the adsorbed interaction parameter. The surface coverture grade, θ, was calculated with inhibition efficiency obtained values, η, and following Equation (7):

$$\theta = \frac{\eta}{100} \qquad (7)$$

Table 3 shows the calculated values through experimental data of *B. arborea* as corrosion inhibitor for 1018 in acid media. The slope obtained from the straight line equation corresponds to the Frumkin model experimental data fitting and with the use of the fitting linear

correlation coefficient R^2; the adsorption constant K_{ads} was calculated through the slope inverse and the standard Gibbs free energy ΔG^0_{ads} was obtained with Equation (8):

$$\Delta G^0_{ads} = -RT \; ln(K_{ads}) \qquad (8)$$

From Gibbs free energy ΔG^0_{ads} the interaction and the adsorption type of the molecules onto the metal surface can be characterized. Generally, ΔG^0_{ads} values up to -20 kJ mol^{-1} are typically correlated to a physisorption and indicates that interactions are electrostatic between organic molecules and charged surface metal; meanwhile values around or higher than -40 kJ mol^{-1} are associated with chemisorption, as a result of electron transfer form organic molecules to the metal surface forming coordinate-type bonds (51, 52).

ΔG^0_{ads} calculated values for *B. arborea* acetone and methanol extracts were -8.01 and -6.1 kJ mol^{-1}, respectively; thus they show a physisorption process; where compounds that contain nitrogen atoms are easily adsorbed onto the surface, due to a pair of free electrons, blocking or decreasing the interaction between the acid media and the steel, as a result, the corrosion speed rate decreases (53).
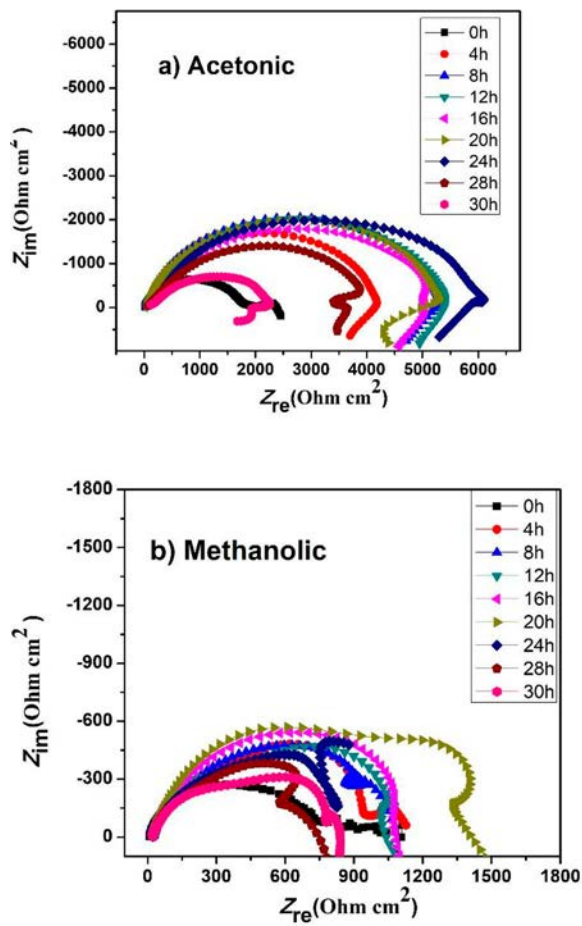
Figure 5. EIS residence time of *B. arborea* extracts at 500 ppm on AISI 1018 carbon steel in 0.5 M H_2SO_4 at 25 °C. (a) Acetonic and (b) methanolic.
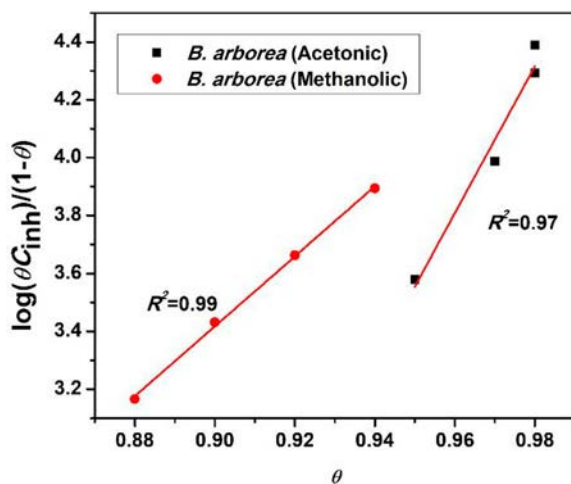

Figure 6. Frumkin adsorption isotherms from AISI 1018 carbon steel in 0.5M of H_2SO_4 using *B. arborea* as green inhibitor

Table 3. Data of the standard Gibbs free energy of adsorption for *B. arborea* extract on AISI 1018 carbon steel in acid medium.

B. arborea extract	Slope	R^2	K_{ads}	$-\Delta G^0_{ads}$ [kJ mol^{-1}]
Acetone	25.36	0.97	0.0394	−8.01
Methanol	12.07	0.99	0.0828	−6.1

3.4. Toxicity bioassay using Lactuca sativa as sensitive organism

Plant bioassays are being more used as they constitute an excellent tool in the environmental evaluation (54). Here, different inhibitor concentrations were used in the germination and growth of *L. sativa* seedlings during its first day of growth. The relative germination percentage (*RG*) and the root relative growth (*CR*) were calculated according to Equations (9) and (10):

$$RG = \frac{n_1}{n_2} * 100 \tag{9}$$

$$CR = \frac{e_1}{e_2} * 100 \tag{10}$$

where n_1 and n_2 are the numbers of germinated seeds in the sample and negative control, e_1 and e_2 are the radicle elongation in the sample and in the blank, respectively.

Figure 7 shows the obtained results for phytotoxicity evaluation for *B. arborea* extracts, where *IG* was determined following Equation (11):

$$IG\% = \frac{RG*CR}{100} \tag{11}$$

There are three classifications to describe the germination index (*IG*) of *L. sativa* seeds under organic substance influence, severe when $IG \leq 50\%$ indicating the presence of strong phytotoxic substances, moderate if $50\% \geq IG \leq 80\%$ and minimum when $IG \geq 80\%$ which is related to the presence of almost null phytotoxic substances.

For *B. arborea* hexane extract *IG* was under 50%, being thus classified as a severe toxic substance; due to this reason and considering its low solubility in the medium, this extract was taken away as an ecological possible inhibitor; also, because the *IG* decreases by
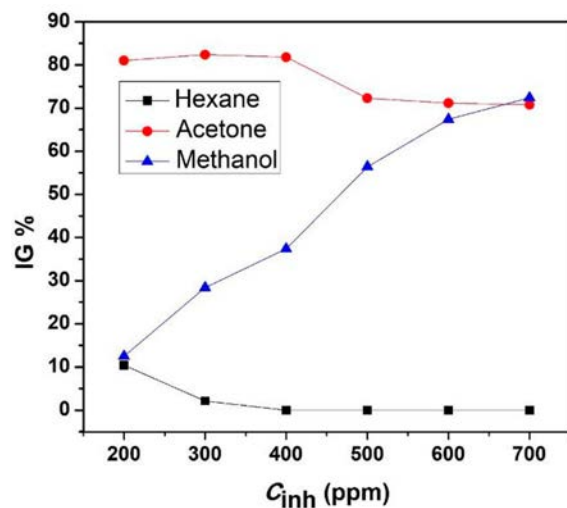

Figure 7. Phyto-toxicity evaluation for *B. arborea extracts*

increasing the presence in the aggressive medium. The best efficiency as corrosion inhibitor, evaluated using PDP and EIS, was from 400 ppm of acetone extract, where the *IG* values were around 50% and 80%, classifying *B. arborea* acetone extract as a substance moderately toxic. On the other hand, the *IG%* values for methanol extract were above 80%, classifying it as a slightly toxic substance.

Most of the studies that talk about green corrosion inhibitors don't show their respective toxicity studies. It is important to determine this as the main theme is green-inhibitor; by using vegetal specie, it not assures that there will be no consequences to the environment or being toxic. Thus, it was demonstrated that by studying the three different extract of *B. arborea,* methanol extract is the greenest to use.

3.5. Infrared spectroscopy by Fourier Transform (FTIR)

Figure 8 shows the spectra obtained by FTIR for the different extracts of *B. arborea,* where vibrational bands assigned to nitrogenous compounds can be observed.

The three extracts showed spectral vibrations in the infrared region, which is characteristic of alkaloid compounds, because in most of them stretching vibrational frequencies can be distinguished for bonds that have nitrogen atoms, such as C–N, N–C, N–CH$_3$, N–H, C = N (55–57). The other signals enable to distinguish double bonds between carbon that are characteristic of aromatic systems and double bonds carbon–oxygen of carbonyl systems. In the same way, it is possible to distinguish spectral vibrations in methanol extract with characteristics of tropane alkaloids, such as scopolamine (58). The vibrations that distinguish tropane compounds are: N-CH$_3$ (950 cm^{-1}), C–N (1175 cm^{-1}), an intense signal at 1708 cm^{-1}, which corresponds to a double bond C = N and the stretching signal at 3575 cm^{-1} (stretching N–H) that is complemented with a vibration at 700 cm^{-1}

3.6. Metallic surface analysis by scanning electron microscope (SEM)

Figure 9 shows the micrographs obtained by SEM, where the metal surface without inhibitor is more deteriorated and with corrosion products. These products did not form a compact layer and the mass loss is visible.

In the case where *B. arborea* acetone extract was used, a compact layer generated by corrosion products and a less deteriorated surface is observed compared to the samples where no inhibitor was used.

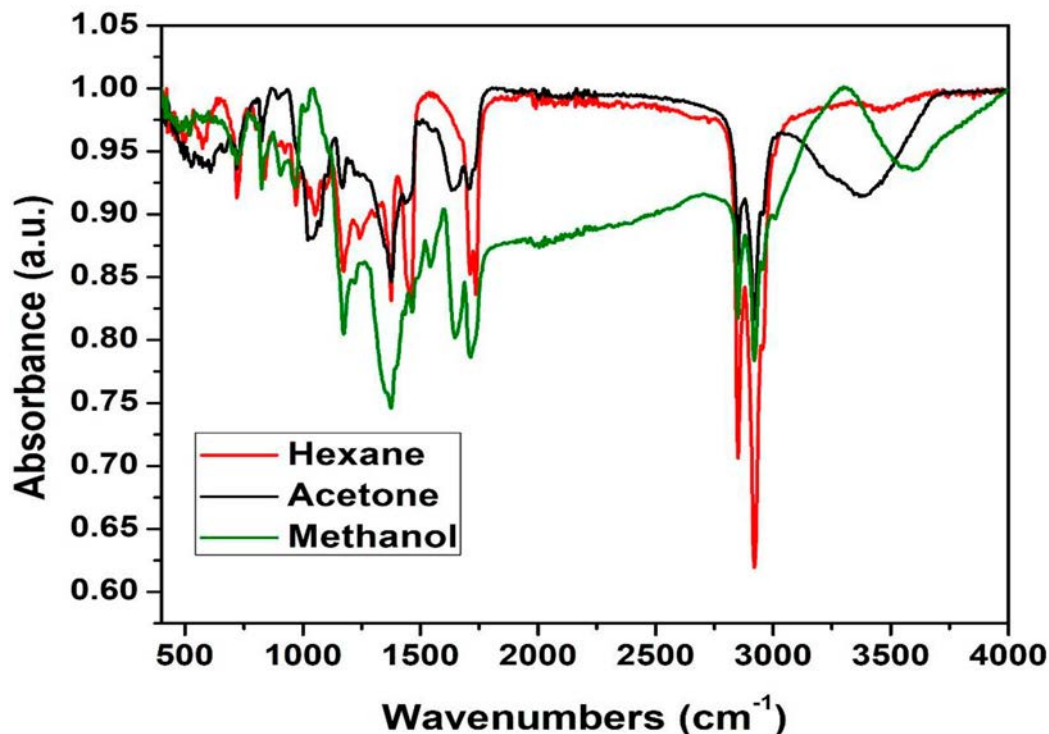In the metal surface where methanol extract was used, a less deteriorated surface compared with the

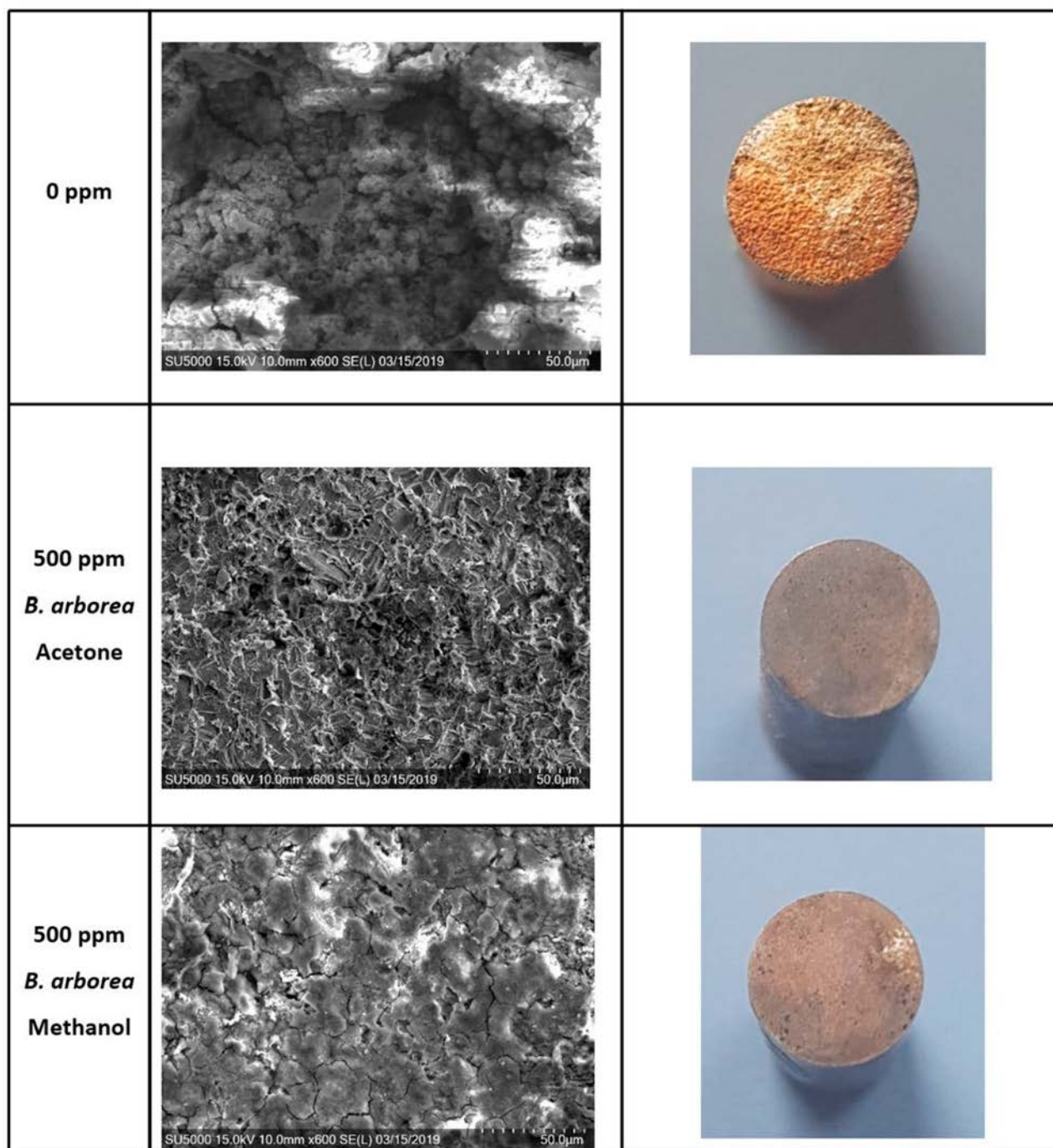**Figure 8.** Infrared spectroscopy spectrums of *B. arborea* extracts

Figure 9. SEM micrographs from AISI 1018 carbon steel in 0.5 M H_2SO_4 at 25°C, without and with 500 ppm *B. arborea*.

blank was observed. However, it has a porous and cracking surface, compared with the surface treated with acetone extract.

4. Conclusions

B. arborea extracts had good inhibition efficiencies (above 80% and 90%) obtained with PDP and EIS techniques for 400 and 500 ppm concentrations respectively. According to Tafel slopes, extracts may be classified as cathodic type inhibitors. Toxicity tests showed that hexane extract is a highly toxic substance; therefore, it was taken away as a possible corrosion inhibitor. Inhibition efficiency increases until 24 h for acetone extract and 20 h for methanol extract, reaching a maximum of 98%. The inhibition efficiency is attributed to the nitrogen compounds present in *B. arborea,* which might be forming complexes that are adsorbed onto the metallic surface, blocking the way of the aggressive species in the medium.

This article presents relevant results around this inhibitor; however, we continue developing it by identifying which are the inhibition responsible compounds and trying its efficiencies individually, as well as doing the studies in dynamic conditions in order to get close to an application.

Disclosure statement

No potential conflict of interest was reported by the author(s).

References

[1] Raichev, R.; Veleva, L.; Valdez, B. *Corrosión de metales y degradación de materiales (In Spanish)*; CINVESTAV: Yucatán, 2009.

[2] Otero, H.E. *Corrosión y degradación de materiales (In Spanish)*; Síntesis: Madrid, 2001.

[3] Sastri, V.S. *Corrosion inhibitor principles and applications*; John Wiley: New York, 1998; pp 39.

[4] Arab, S.T.; Noor, E.A. *Corros. Sci.* **1993**, *49* (2), 122–129.

[5] Mernari, B.; El Attari, H.; Traisnel, M.; Bentiss, F.; Lagrenee, M. *Corr. Sci.* **1998**, *40*, 391–399.

[6] Al-Kharafi, F.M.; Al-Hajjar Farouk, H. *J. Univ. Kuwait* **1992**, *19*, 61–75.

[7] Stupnisek-Lisac, E.; Lončarić Božić, A.; Cafuk, I. *Corrosion* **1998**, *54*, 713–720.

[8] Quraishi, M.A.; Khan, M.A.W.; Ajmal, M.; Muralidharan, S.; Iver, S.V. *Corrosion* **1997**, *53*, 475–480.

[9] Sahin, M.; Gece, G.; Karci, F.; Bilgic, S. *J. Appl. Electrochem.* **2008**, *38*, 809–815.

[10] Hassan, K.H.; Khadom, A.A.; Kurshed, N.H. *S. Afr. J. Chem. Eng.* **2016**, *22*, 1–5.

[11] Mendoça, S.A.; Almeida, T.F.; Cotting, F.; Aoki, V.I.; Melo, H.G.; Capelossi, V.R. *Mater. Res.* **2017**, *20*, 492–505.

[12] Yaro, A.S.; Khadom, A.A.; Wael, R.K. *Alexandria Eng. J.* **2013**, *52*, 129–135.

[13] Philip, J.Y.N.; Buchweshaija, J.; Mwakalesi, A. *Mater. Sci. Appl.* **2016**, *7*, 396–402.

[14] Al-Fakih, A.M.; Aziz, M.; Sirat, H.M. *J. Mater. Environ. Sci.* **2015**, *6*, 1480–1487.

[15] Rodríguez-Clemente, E.; González-Rodríguez, J.G.; Valladares-Cisneros, M.G.; Chacon-Nava, J.G. *Green Chem. Lett. Rev.* **2015**, *8*, 49–58.

[16] Prabakaran, M.; Kim, S.; Hemapriya, V.; Gopiraman, M.; Kim, I.S.; Chung, I. *RSC Adv.* **2016**, *6*, 57144–57153.

[17] Haldhar, R.; Prasad, D.; Saxena, A.; Singh, P. *Mater. Chem. Front.* **2018**, *2*, 1225–1237.

[18] Okewale, A.O.; Olaitan, A. *Int. J. Mat. Chem.* **2017**, *7*, 5–13.

[19] Guillot-Ortiz, D.E. *Flora ornamental española: aspectos históricos y principales especies (In Spanish)*; Bouteloua: España, 2009.

[20] Wang, X.R.; Chen, M.; Yang, C.X.; Liu, X.Q.; Zhang, L.; Lan, X.Z.; Tang, K.X.; Liao, Z.H. *Physiol. Plant.* **2011**, *143*, 309–315.

[21] Qiang, W.; Xia, K.; Zhang, Q.; Zeng, J.; Huang, Y.; Yang, C.; Chen, M.; Liu, X.; Lan, X.; Liao, Z. *Phytochemistry* **2016**, *127*, 12–22.

[22] Abdallah, M.; Helal, E.A.; Fouda, A.S. *Corros. Sci* **2006**, *48*, 1639–1654.

[23] Sobrero, M.; Ronco, A. In: *Ensayos toxicológicos y métodos de evaluación de calidad de aguas*; Castillo, G. Ed.; IMTA: México, 2004; Chapter 4.

[24] Veloz, M.A.; González, I. *Electrochim. Acta* **2002**, *48*, 135–144.

[25] Kelly, E.J. *J. Electrochem. Soc.* **1965**, *112*, 124–131.

[26] Hurley, B.L.; Ralston, K.D.; Buchheit, R.G. *J. Electrochem. Soc.* **2014**, *161*, 471–475.

[27] Morad, M.S. *J. Appl. Electrochem.* **1999**, *29*, 619–626.

[28] Shukla, S.K.; Quraishi, M.A.; Ebenso, E.E. *Int. J. Electrochem. Sci.* **2011**, 6, 2912–2931.

[29] Fawcett, W.R.; Kovacova, Z.; Motheo, A.J.; Foss, C.A. *J. Electroanal. Chem.* **1992**, *326*, 91–103.

[30] Priyotomo, G.; Nuraini, L. (2016) In: Seminar Nasional Metalurgi dan Material, Proceeding of SENAMM IX. Cilegon, Indonesia, Oct 11, 2016.

[31] Bentiss, F.; Lagrenee, M.; Traisnel, M.; Hornez, J.C. *Corros. Sci.* **1999**, *41*, 789–803.

[32] Brett, C.M.A. *J. Appl. Electrochem.* **1990**, *20*, 1000–1003.

[33] Sun, C.; Delnick, F.M.; Aaron, D.S.; Papandrew, A.B.; Mench, M.M.; Zawodzinski, T.A. *J. Electrochem. Soc.* **2014**, *161*, 981–988.

[34] Behpour, M.; Ghoreishi, S.M.; Mohammadi, N.; Soltani, N.; Salavati-Niasari, M. *Corros. Sci.* **2010**, *52*, 4046–4057.

[35] Haruyamas, S.; Asari, M.; Tsuru, T. (1987) In: *Proceedings of the Symposium on Corrosion Protection by Organic Coatings*, Kendig MW, Leidheiser H (Eds), 1st ed. The Electrochemical Society, Pennington.

[36] Kending, M.; Jeanjaquet, S.; Brown, R.; Thomas, F. *J. Coat. Technol.* **1996**, *68*, 39–47.

[37] Özkır, D.J. *Electrochem. Sci. Technol* **2019**, *10*, 37–54.

[38] Döner, A.; Altunbaş Şahin, E.; Kardaş, G.; Serindağ, O. *Corros. Sci.* **2010**, *66*, 278–284.

[39] Díaz Cardenas, M.Y.; Valladares, M.G.; Lagunas Rivera, S.; Salinas Bravo, V.M.; Lopez Senses, R.; Gonzalez Rodríguez, J.G. *Green Chem. Lett. Rev.* **2017**, *4*, 257–268.

[40] Arenas, M.A.; Damborenea, J.J. *Revista de metalurgía* **2006**, *42*, 165–174.

[41] Aldana Gonzalez, J.; Espinoza Vazquez, A.; Romero Romo, M.; Uruchurtu Chavarin, J.; Palomar Pardave, M. *M Arabian J. Chem.* **2015**. doi:10.1016/j.arabjc.2015.08.033

[42] Ghanbari, A.; Attar, M.M.; Mahdavian, M. *Mater. Chem. Phys.* **2010**, *124*, 1205–1209.

[43] Nwabanne, J.T.; Okafor, V.N. *JMMCE* **2012**, *11*, 885–889.

[44] Seifzadeh, D.; Basharnavaz, H.; Bezaatpour, A. *Mater. Chem. Phys.* **2013**, *138*, 794–802.

[45] Aljourani, J.; Raeissi, K.; Golozar, M.A. *Corr. Sci.* **2009**, *51*, 1836–1843.

[46] Stupnisek-Lisac, E.; Salajster, K.; Furac, J. *Corros. Sci.* **1988**, *28*, 1189–1202.

[47] Singh, A.; Ebenso, E.E.; Quraishi, M.A. *Int. J. Electrochem. Sci* **2012**, *7*, 8543–8559.

[48] Pal, S.; Lgaz, H.; Tiwari, P.; Chung, I.; Ji, G.; Prakash, R. *J. Mol. Liq.* **2019**, *276*, 347–361.

[49] Loto, R.T. *J. Fail. Anal. Preven.* **2017**, *17*, 1031–1043.

[50] Bouyanzer, A.; Hammouti, B.; Majidi, L. *Mater. Lett.* **2006**, *60*, 2840–2843.

[51] Ammar, I.A.; El Khorafi, F.M. *Mater. Corros.* **1973**, *24*, 702–707.

[52] El Guerraf, A.; Titi, A.; Cherrak, K.; Mechbal, N.; El Azzouzi, M.; Touzani, R.; Hammouti, B.; Lgaz, H. *Surf. Interfaces* **2018**, *13*, 168–177.

[53] Al-Turkustania, A.M.; Araba, S.T.; Al-Qarnib, L.S.S. *J. Saudi Chem. Soc.* **2011**, *15*, 73–82.

[54] Chan Keb, C.A.; Agraz Hernández, C.M.; Perez Balan, R.A.; Gómez Solano, M.I.; Maldonado Montiel, T.D.N.J.; Ake Canche, B.; Gutiérrez Alcántara, E.J. *Toxicol. Rep.* **2018**, *5*, 593–597.

[55] Belen'kii, L.I.; Evdokimenkova, Y.B. *Adv. Heterocycl. Chem.* **2014**, 132, 111–147.

[56] Gunasekaran, S.; Ponnusamy, S. *Indian Jounal Pure Appl. Phys.* **2005**, *43*, 838–843.

[57] Lounasmaa, M.; Tamminen, T. (1993) In: *The Tropane Alkaloids*, Brossi A (Ed) 1st ed. Academic Press, New York.

[58] Welegergs, G.G.; Hulif, K.; Mulaw, S.; Gebretsadik, H.; Tekluu, B.; Temesgen, A. *Science Journal of Chemistry* **2015**, *3*, 78–83.